A COMPARISON OF INJURY CRITERIA USED IN EVALUATING SEATS FOR WHIPLASH PROTECTION

Allan F Tencer, Sohail Mirza, Philippe Huber
Orthopedic Sciences Laboratory
Department of Orthopedics,
University of Washington,
Seattle, Washington,
United States
Paper No 99

ABSTRACT
A protocol has been proposed for testing seats for whiplash protection, however injury criteria were not chosen. Assuming that whiplash symptoms arise from non-physiological motions of vertebral segments, we determined the ability of proposed criteria to predict peak individual vertebral displacements. Volunteers were subjected to rear impacts while seated in a car seat with head restraint, mounted onto a sled. Then, the seat was replaced by a platform onto which were mounted cadaveric cervico-thoracic spines. Head and T1 accelerations and individual vertebral sagittal (XZ) plane rotations and translations were obtained. Proposed injury criteria were tested for their ability to predict peak intervertebral displacements. Cadaveric specimens had chest and head X (horizontal) and Z (vertical) linear accelerations similar to volunteers whose heads hit the head restraint. The best predictors were: Nd shear and peak posterior translation (0.80), Nd extension and peak extension angle ($r^2 = 0.70$), and Nd distraction and peak distraction (0.51). Therefore consideration should be given to a displacement based injury criteria such as Nd.

INTRODUCTION

An average of 805,581 whiplash injuries occurred annually in the United States from 1988 to 1996, with an estimated cost of $5.2 billion dollars [1]. Whiplash may result in a chronic condition, though its diagnosis is often confounded by a general lack of objective symptoms [2-5]. Since whiplash derives from the occupant's response to the forces applied during a rear impact, the intersegmental displacements of the cervical vertebrae and tissue deformations resulting from abnormal motions most probably produce whiplash symptoms. Since testing of new devices to prevent whiplash is performed with crash dummies, spinal intersegmental motions and tissue deformations cannot be readily determined. Injury parameters, measurable from the dummy, have therefore been used to predict whiplash injury.

In this study we measured intersegmental motions in cadaveric specimens and correlated these motions to injury parameters proposed in the literature, to determine the best predictors of vertebral motions.

The response of an occupant to a rear-end impact has been well documented [6-20]. During the collision the vehicle and seat are pushed towards the occupant. The occupant's torso contacts the seat back first, and is thrust forward underneath the momentarily stationary head. The head retracts and extends rearward, contacting the head restraint, resulting in cervical spine shearing, tension, and extension. At this point the vehicle-to-vehicle impact is over. The occupant's torso continues to move forward, and the head starts to rebound forward from the head restraint. The torso forward motion is stopped by the shoulder belt while the head continues forward over the torso flexing the neck. The shoulder and lap belt arrest the occupant's torso and he or she falls back into the seat. Several recent studies, most performed using cadaveric cervical spine preparations, have identified an initial transient "S" shape to the cervical spine in response to a rear-end impact due to the lower cervical spine being thrust forward with the torso by the seat while the head and upper cervical vertebrae remain initially stationary due to the inertia of the head. This "S" shape was related, in different reports, to nonphysiologic extension of the lower cervical segments [14], pinching instead of gliding of the facets [6,13], increased facet capsular tissue strains [7], and transient compression of the neural tissues [8]. Any or all of these nonphysiologic vertebral intersegmental deformations may account for symptoms experienced by victims of rear impact. All of these tissue related strains result from abnormal kinematics of the cervical vertebrae.

Recently, a protocol has been proposed for testing seats and head restraints [21] however, the authors stated that more work was required to validate criteria for whiplash injury risk. A number of injury parameters and thresholds have been proposed for whiplash injury. Bostrom, et al [22] defined NIC, the neck injury criteria, which is calculated from the acceleration and velocity of the head in relation to the neck. Schmitt, et al [23] proposed Nkm based on neck shear force and flexion/extension moment. Viano and Davidsson [24] suggested Nd which considers head rotation at the occipital condyles, and occipital condyle to T1, along with X (shear) and Z (tension-compression) displacements. Kleinberger, et al [25] used Nte a subset of the Nij criterion which considered both extension moment and neck tensile force. Jacobson and Norion [26], suggested using

head rebound velocity along with some of the previously proposed criteria. The goal of our study was to determine how the criteria proposed by others correlated with spinal peak intersegmental motions that were measured using cadaveric cervical spines subjected to rear impacts. The results suggest which of the proposed criteria may best predict abnormal cervical spinal kinematics and indirectly, the potential for whiplash injury.

METHODS

Study Design and Limitations

The general setup is described here and details are given in following paragraphs. Data from a set of 26 human volunteer rear impact experiments [20] was used to develop response corridors for occupant head and sternum accelerations. Using the same crash pulse time, sled, head restraint, and head to restraint distance (backset), from that study [20] a set of 11 cadaveric spine preparations was tested so that intersegmental motions could be determined at each cervical vertebral level. The weight of the impact pendulum was adjusted until the accelerations at cadaveric spine level T1 were within the corridors for sternum accelerations of volunteers. Cadaveric specimens used were limited to C1-T4 segments with the same instrumented skull replica attached to each. Spinal intersegmental sagittal plane rotations and translations were recorded by high speed video.

Using cadaveric spines has recognizable limitations but were necessary to allow measurement of inter-segmental motions.   Since our cadaveric spines had no supporting musculature, these tests represent the worst case, that of the unprepared occupant. The volunteer tests, by their nature, do not simulate the unaware occupant, so muscle tension may be larger than that exhibited by an unprepared occupant in an actual crash. Considering both volunteers and cadavers probably covers the bounds of the responses due to level of preparedness and resulting neck muscle tension.

Although the complete thoracic spine was not present in the cadaveric tests, there were a sufficient number of mobile segments to observe straightening of the spine and resulting vertical head accelerations, similar to those described in volunteer studies. The sternum accelerations of cadaveric specimens were matched to those observed by volunteers. This is probably the best indicator that the interaction of the seat with the torso of the volunteer was being

replicated in our cadaver experiments, in which the head restraint was present, but not the seat.

We chose to attach the same instrumented replica of a skull to each specimen instead of maintaining the head of the specimen. Since head weight affects cervical spines forces in rear impact, this resulted in smaller variations in responses while allowing us to instrument the head replica with the same accelerometers for all tests. All cervical joint motions were maintained. No joints were fused or altered by attachment of the head replica.

Volunteer testing

One of the 19 seats previously tested for impact properties [20] was selected as having midrange stiffness and energy absorption properties. It was mounted on a 6 wheeled sled running inside guide rails and had an impact absorbing bumper constructed of two aluminum channels separated by two sets of rubber doughnuts. Energy was provided by the same pendulum used to test the seats in the prior study but with more weight added (total pendulum mass was about 73 kg). Its drop height produced a velocity of the pendulum at impact of about 6.4 kph (4 mph) and bumper compression resulted in an impact with an acceleration rising linearly to a peak of about 2.5g in about 66 msec, Fig 1, followed by a deceleration
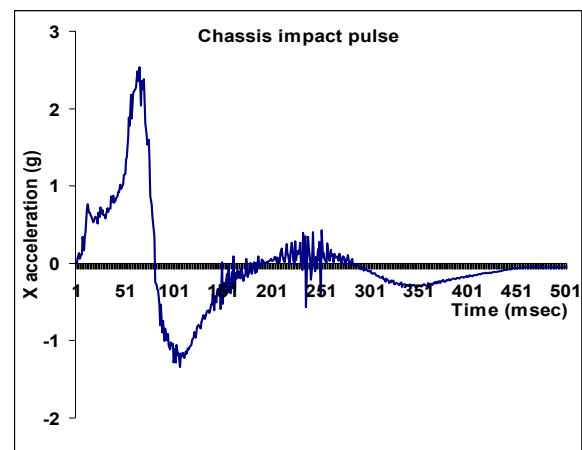

Figure 1. Mean input acceleration pulse in volunteer testing, including deceleration of sled by frictional contact with rails.

reaching a peak of –1.3g at 103 msec due to frictional interaction of the wheels of the sled with the frame rails. Overall the sled traveled about 40 cm after impact reaching a peak velocity of 3.9 kph. This represented both the acceleration and deceleration components in a rear end impact against a stopped vehicle with the brakes applied. Testing was

vehicle with the brakes applied. Testing was performed with the approval of the Institutional Review Board of the University of Washington. A total of 28 subjects were tested from which 26 intact data records were analyzed. The subjects were recruited from hospital employees and included 14 females (age range 22-64 yrs) and 12 males (age range 28 to 50 years). Each subject was seated in the sled, shown in Figure 2, and restrained with lap and shoulder belts. A light plastic headband was secured on the subject's head with an elastic strap under the chin. It contained 5 accelerometers (PCB Piezotronics Inc, Depew, NY), 2 uniaxial, measuring X (forward-backward) and Z (upward-downward) accelerations at approximately the level of each ear, and one triaxial, located at the apex of the head forming a vertical plane with the accelerometers at both ears. The accelerometers at ear level were located approximately at the estimated center of gravity of the volunteer's head, in the sagittal plane [12,28].

In a previous study [19], the motions of the head and chest of volunteers in simulated rear-end impacts were observed to occur primarily in the X (forward-backward) and Z (upward-downward) directions or in the sagittal plane, so only X and Z accelerations were measured in this study. Signals were sampled using a laptop computer (Powermac G3, Apple Computer Co, Cupertino, CA) with an A/D card and software (Labview, National Instruments, Austin, TX) and were filtered according to SAE J 211 using a 5th order 4 pole Butterworth digital filter implemented in Labview. The instrumentation on the head was located on the same rigid body, however the head translated and rotated in the XZ (sagittal) plane. The resultant motion at each of the three measurement locations was independent of the orientation of the accelerometers (the local coordinate system) since the resultant can be expressed in an infinite number of coordinate systems. To describe the translation and rotation of the subject's head in the XZ plane, it was transformed into a translation with reference to the lower part of the ear near the TMJ joint and an XZ plane rotation about this point. The actual origin for each accelerometer pair was at the intersection of the axes of the X and Z accelerometers.

Cadaveric testing

Fresh frozen cadaveric preparations were thawed and dissected into a cervical and upper thoracic spine unit. Muscle and soft tissues were removed maintaining the discs, facet capsules, and ligaments intact. Each spine was examined by manual palpation and with lateral and AP radiographs. Two experienced observers used the radiographs to score disc degeneration at each level in the cervical spine, with the following grades; Grade 1: end plate (EP) uniform thickness, vertebral body (VB) rounded margins, Grade 2, EP irregular thickness, VB pointed margins, Grade 3, EP focal defects, VB chondrophytes, Grade 4, EP fibrocartilage, VB < 2mm osteophytes, Grade 5, EP diffuse sclerosis, VB > 2mm osteophytes, [29]. A mean score for each spine, averaging scores for each level, was determined. Those with significantly restricted, degenerated, or hypermobile segments were not used. Eleven cervico-thoracic specimens were selected from a total of 16 available. Table 1 lists the characteristics of the specimens.

The sled previously used for testing volunteer response to rear-impact [20] was modified by removing the seat and replacing it with a frame and platform. The sled frame, bumper, wheels and guide rails remained unaltered from the volunteer experiment. The head restraint of the seat used in that experiment was mounted onto the platform, shown in Figure 3. The lower end of the specimen was firmly mounted in a clamping box with rubber pads contacting the thoracic vertebrae. This arrangement was used because in prior (unpublished) work where the thoracic spine was fixed in a rigid material, it was observed that a high stress concentration developed and the spine fractured at the junction between the
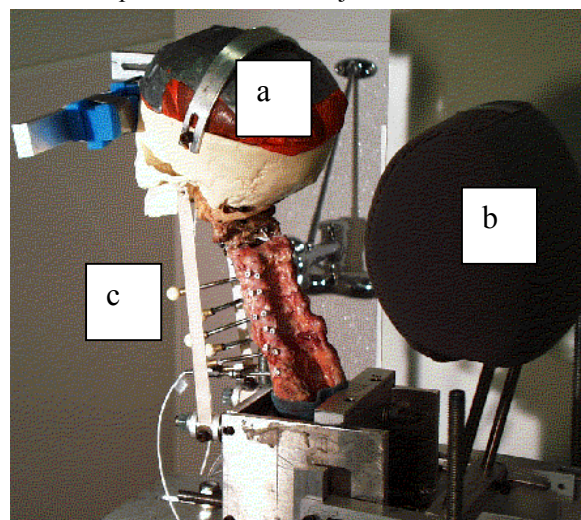

Figure 3. Cadaveric test arrangement showing (a) skull replica attached to cervical spine, (b) head restraint, (c) vertebral and lateral mass video markers on C3-T1.

unsupported and the fixed regions. A load cell (WSM Industries, Inc) mounted under the specimen mounting box was used to measure spinal shear force during impact. A plastic replica of a human skull (Anatomical Chart Co, Skokie, IL) was instrumented with a triaxial accelerometer (Kistler Instrument Corp, Amhurst, NY) placed at its estimated center of gravity and was filled with jelly to mimic the weight and mass distribution of the brain. The center of gravity had been determined by balance weighing of the skull. The plastic skull was attached to a segment of bone remaining from the base of the skull of the specimen. All cervical spinal joints remained intact. Using a standardized plastic skull removed some variability from responses of the specimens due to different head weights and allowed the use of a head mounted accelerometer. A stop was placed forward of the head to prevent excessive forward motion after impact since no muscles were available to control and arrest head motion.

Local vertebral kinematics were determined from high speed video (Kodak, EktaPro, Rochester, NY) of markers placed onto each vertebra, from C3 to T1, taken at 1000 frames/sec. Pins placed anteriorly into each vertebral body were used to determine vertebral orientation and two 3.5 mm screws placed into each lateral mass allowed determination of facet orientation and relative displacement, Figure 3. Imaging software (WINanalyze Mikromak GmbH, Erlangen, Germany), accurate to 0.01 pixels, was used to determine marker coordinate positions in the video frames. This analysis was limited to the sagittal plane. Vertebral intersegmental angulation and facet displacements were determined. A marker was filmed in each video and was used for calibration.

By adjusting the weight of a pendulum, to 267N, and raised to a height of about 38 cm, a chest acceleration, detected by a uniaxial accelerometer mounted to the body of vertebra T1 of the specimen, was generated that was similar to accelerations detected at the sternums of volunteers in a previous study [20], Figure 4. Head acceleration was detected by the triaxial accelerometer mounted in the skull. Shear force was determined by a transducer mounted between the base of the specimen mounting box and the platform of the sled. Sampling was performed at 3 KHz using a laptop computer (Macintosh Powerbook G3, Apple Computer Co, Cupertino, CA) with an analog to digital signal card and Labview software (National Instruments Co, Austin, TX). The accelerometer data was forward and reverse filtered using a 5 pole Butterworth filter implemented in Labview.
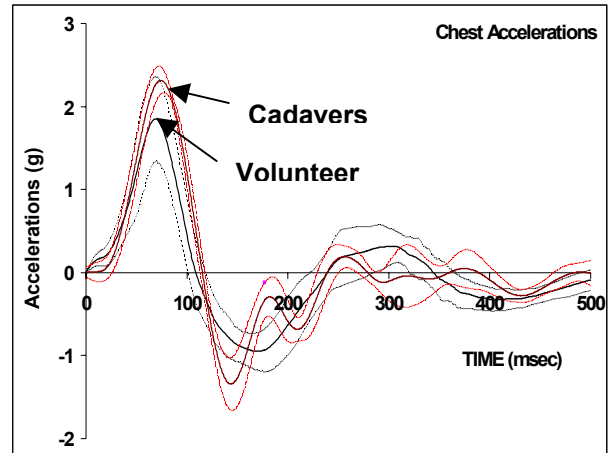

Figure 4. Forward (X) accelerations of volunteers, at the sternum, (n = 26, +/- 1 sd) and cadavers, at T1 (N = 11, +/- 1 sd).

The head restraint from the previous volunteer study [20], was mounted about 4 cm behind the skull. A switch triggered a high speed video camera and the data collection system just before the pendulum impacted the sled bumper. After head rebound from the head restraint, a stop was used to prevent excessive forward excursion of the head. After the first test, at about 2g peak chest acceleration, the head restraint was moved backward until the head-to-restraint gap was doubled to about 8 cm (twice that of the volunteer tests) and the impact repeated. Then, the head-to restraint distance was decreased to 4 cm, and the pendulum weight increased to 1068N. The impact was repeated, doubling the chest acceleration to about 4g. The head restraint was removed and replaced with a different head restraint. Finally, to determine whether whiplash testing had altered the properties of the spine being measured, the pendulum weight was decreased to 267N, the standard head restraint put back in place, and the lower acceleration test, similar to the first test, was performed. Varying the test conditions for each specimens increased the data available for correlation.

Calculation of injury criteria

Injury criteria were calculated as described in the literature. NIC is a criteria using relative acceleration and velocity of T1 with respect to the head and is based on the hypothesis that these relative kinematics induce injurious pressures in spinal neural tissues. NIC was determined from [22]:

NIC (t) = 0.2 $* A_{rel}$ (t) + $(V_{rel})^2$, where,   (1).

A_{rel} (t) = A_{T1X} (t) - A_{headX} (t)
V_{rel} (t) = integral $(A_{rel}(t)$ dt)

Both minimum and maximum NIC values were used.

N_{te} is part of the general Nij criterion and considers the combination of neck extension moment and tensile force during the extension phase of the rear impact. It was calculated by [25]:

N_{te} = (F_z/F_{crit}) + (M_{ext}/M_{crit}), where,   (2).
  F_{crit} = 3600 N
  M_{crit} = 125 N-m
  F_z = W_h * A_z (N)
  A_z = peak z acceleration of head (g)
  W_h = head weight = 42.15N
  M_{ext} = SQRT $(F_z^2 + F_x^2)$ * r
  Fx = Wh *A_x (N)
  A_x = peak x acceleration of head (g)
  r = head cg to occipital condyles dist = 0.076m

N_{km} is a modification of the approach of combining both force and moment but uses shear force instead of tensile force. It was calculated by [23]:

N_{km} (t) = F_x (t) / F_{int} + M_y (t) / M_{int}, where,   (3).
  F_{int} = maximum shear force, 845 N
  M_{int} = 47.5 N-m, extension
  M_y = Mext   (N-m)

Nd considers maximum displacements instead of forces [24]. To provide numerical values, it was modified to allow calculation of ratios as with Nte and Nkm, and was computed from:

Nd total = Nd ext + Nd shear + Nd dist,   (4).
 where,

Nd angle = Θ_{oc}/Θ_{oc} max extension
Nd shear = X_{oc-T1}/X_{oc-T1} max
Nd distraction = Z_{oc-T1}/Z_{oc-T1} max, and

  Θ_{oc} max < 25°
  X_{oc-T1} max < 35 mm
  Z_{oc-T1} max < -15 mm

RESULTS

Volunteer and cadaveric head accelerations
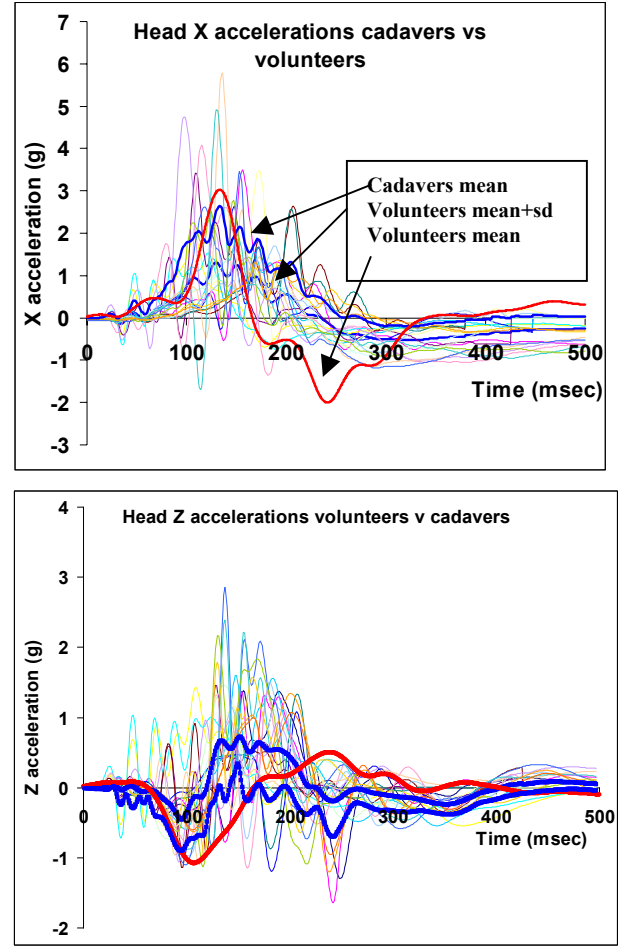
Figure 5 Head acceleration (g) vs time (msec) (upper) individual X traces for volunteers, and mean X accelerations with corridors, +/- 1 sd (blue), and cadavers mean (red), (lower) mean Z accelerations

The comparisons of head accelerations from cadaveric tests at the approximate c.g of the head, (identical head restraint, 4cm head-to-restraint gap) and volunteers for the same conditions are shown in Figure 5 for both X and Z directions. The collection of time histories shows the variations among volunteers. Tests in which the volunteer did not hit the head restraint were not used because they indicate significant muscle tensing and preparedness for the impact and it would be unreasonable to compare those tests to cadavers. They also do not simulate the typical crash in which the occupant is unaware and surprised by the impact.

Peak acceleration occurred at about the same time for both volunteers and cadavers but cadaver mean peak acceleration reached about 2.9g while volunteer accelerations (peak + 1 sd) was about 2.6g. In fact, considering only peak acceleration values, disregarding the time at which they occurred, the average peak head cg X acceleration was 2.6g for volunteers. The rebound peak (negative) acceleration was higher for cadavers since the heads of the cadavers all hit the flexion stop, which did not occur in volunteer tests. However, the intervertebral motions, which will be described in the following section, coincided with peak accelerations at the time of head restraint contact, so the rebound phase was not significant for our analysis. Peak Z accelerations in cadavers reached a mean of -1g, while volunteer accelerations (mean -1 sd) were about -0.9g. For both head X and Z accelerations, peaks occurred at similar times for volunteers and cadavers. Although the cadaveric mean accelerations were greater than volunteer mean accelerations, they fell within the mean +/- 1 sd of the volunteer responses and there was no significant difference in mean values. Since there was no attenuation of head motions by muscles in cadaveric specimens, the somewhat higher accelerations were not unexpected. Therefore, the cadaveric tests can be considered to reasonably replicate the kinematics of unprepared volunteers.

Cadaveric intersegmental cervical spine motions during impact

Figure 2 shows representative time history data along with frames from the high speed video of the cadaveric testing, and from a representative volunteer, to demonstrate the position of the head and neck at the time of peaks in the values measured. For this case, the chassis impact acceleration peak occurred at 64 msec, followed by the chest (actually at T1) acceleration, which peaked at about 4.3g at 82 msec. The head acceleration peaked later, 4.9g at 122 msec. Peak accelerations occur when the seat back impacts the back of the torso and the head restraint impacts, at a later time, the back of the head. This time lag probably represents the basic mechanism which causes differential motion across the vertebral segments. At C5-6 a small degree of flexion occurred initially, just as the chest and head accelerations started to rise, then the motion segment extended, with its peak just following the peak head acceleration. The change in intervertebral posterior shear corresponded to the change in extension angulation, with its peak occurring at about the same time as peak head acceleration.
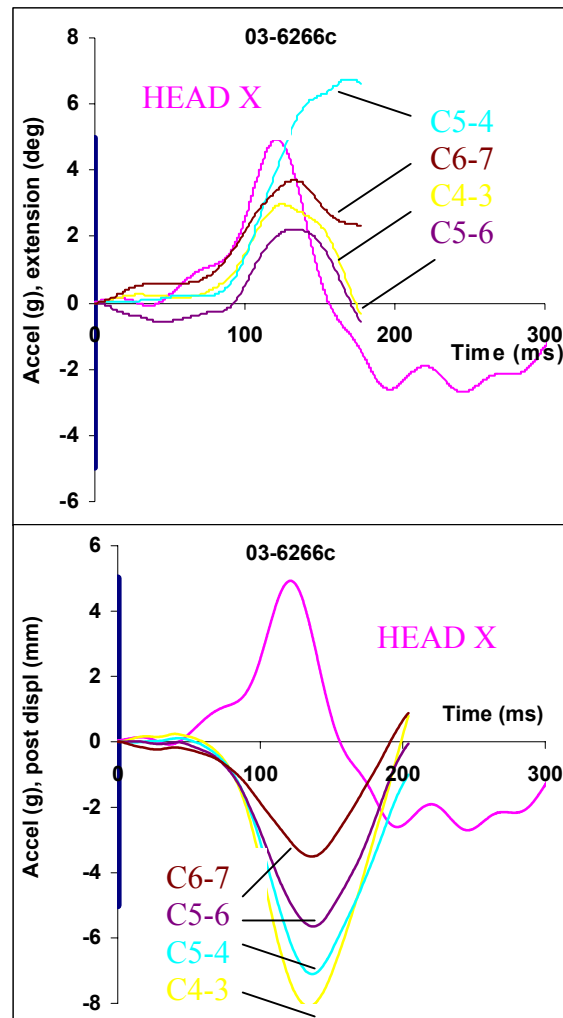
Figure 6 (upper) Comparison of relative flexion (-) and extension (+) angles at each motion segment (lower) intervertebral posterior shear (X) displacements (mm), from one specimen in one test

Figure 6 (upper) demonstrates relative intersegmental motions which occurred in a representative specimen, along with peak head acceleration. There was a considerable difference in magnitude of the posterior shear displacements along the spine, with the greatest, at C3-4, being about double that at C6-7, although all displacements increased and decreased with a similar time course. The reason for the difference, although the bending load of the head was the same along the spine, is that depending on its degree of degeneration, each motion segment had different stiffness. In fact, considering that specimen 3 had greatest degeneration

at levels C5-6 and C6-7 (Table 1) its is not surprising that these levels show the least displacement. As shown in Figure 6 (upper) there was reasonably uniform extension at each motion segment along the spine. Flexion has been described at the head and upper cervical levels, but in this study, C0-1-2 displacements were not measured since is was difficult to place markers at these levels.

Table 2
Correlation coefficients (r^2) between intersegmental displacements, extension angle (deg), posterior shear (mm), distraction (mm), mean, sum or total displacement, peak or maximum value

	POSTERIOR SHEAR			EXTENSION ANGLE			DISTRACTION		
	mean	sum	peak	mean	sum	peak	mean	sum	peak
EXTENSION, mean									
mean	0.001								
sum		0.079							
peak			0.018						
POSTERIOR SHEAR									
mean				0.065					
sum					0.350				
peak						0.037			
DISTRACTION									
mean							0.068		
sum								0.000	
peak									0.007

The different displacements at each intervertebral segment were correlated, using linear regression, to determine whether there were any significant relationships among them. The only two displacements that showed a modest correlation, $r^2 = 0.35$, were total posterior shear (sum of all levels of a specimen) and total extension angle, as shown in Table 2. Therefore the intersegmental displacements were essentially unrelated indicating that a spinal motion segment can have significant shear displacement without much angulation, or distraction without shearing.

Relationship of spinal motions and injury criteria.

Table 3
Correlation coefficients (r^2) between mean, sum or total intersegmental displacements, (extension angle (deg), posterior shear (mm), distraction (mm)), and injury predictors.

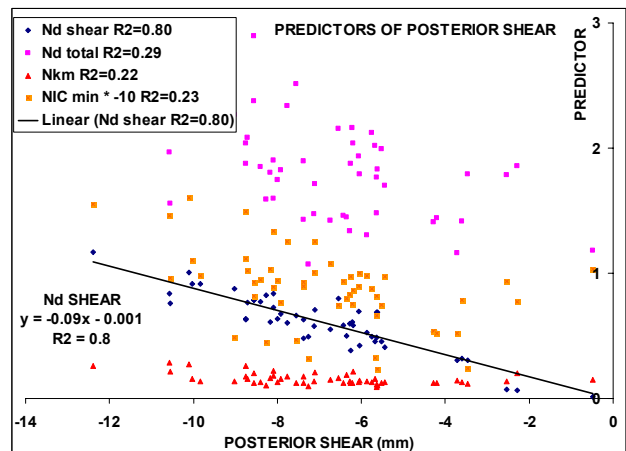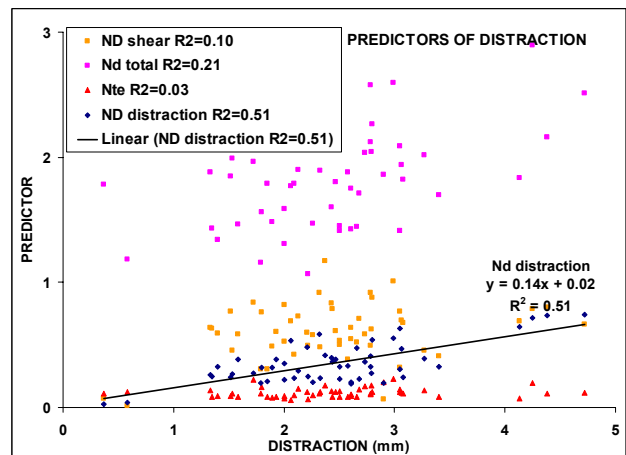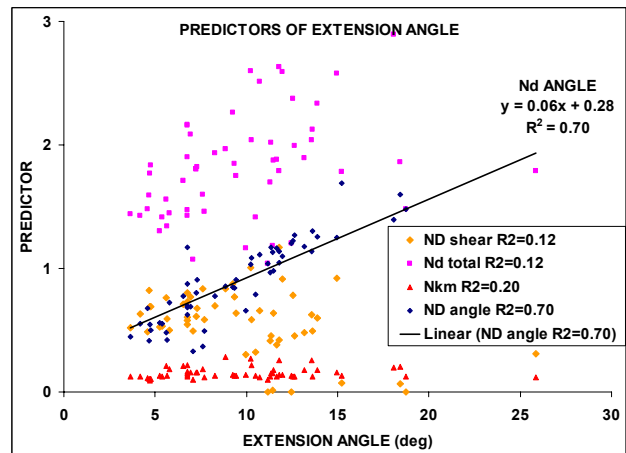|	Posterior shear			Extension angle			Distraction		
	mean	sum	peak	mean	sum	peak	mean	sum	peak
Nd total	0.316	0.305	0.288	0.258	0.219	0.122	0.351	0.380	0.209
Nd shear	0.768		0.800	0.064	0.128	0.122	0.056	0.350	0.096
Nd angle	0.007	0.079	0.015	0.839		0.696	0.047	0.014	0.000
Nd distraction	0.151	0.351	0.147	0.012	0.044	0.040	0.579		0.505
Nte	0.056	0.051	0.118	0.123	0.097	0.067	0.069	0.011	0.031
Nkm	0.149	0.118	0.221	0.036	0.030	0.015	0.006	0.000	0.006
NICMAX	0.206	0.175	0.113	0.001	0.002	0.002	0.048	0.035	0.079
NICMIN	0.151	0.105	0.225	0.051	0.040	0.001	0.023	0.021	0.040

Figure 7 Relationships between injury predictors and (upper) facet posterior shear displacement (mm), (middle) extension angulation (deg), and (lower) facet distraction.

Table 3 provides the linear correlation coefficients that were derived between various injury predictors

and the mean, total or sum, and peak intervertebral displacements. Considering that the peak displacement might indicate the location of injury in a specimen, the best injury criterion for predicting peak posterior shear was Nd shear (r^2=0.800) with significant but poor correlations with Nd total (0.288), NIC min (0.225), and Nkm (0.221). For peak extension angulation, the best correlation was found with Nd angle (0.696) followed by Nd total (0.122) and Nd shear (0.122). For facet distraction, the best correlation was with Nd distraction (0.505) followed by Nd total (0.221). The correlations are presented graphically in Figure 7. All the data used in constructing these relationships is given in Table 4.

DISCUSSION

In this study we addressed the relationship of injury predictors, measurable by crash dummies, and peak intervertebral displacements within the cervical spine. The best predictor for all three peak displacements considered was Nd, a displacement based criteria. The force based criteria probably performed poorly because the displacement response to an applied force, even within the same spine, is quite variable, as shown in Figure 6. As shown in Table 1 there was variation in degeneration at different vertebral levels in each specimen. Although the specimens donors were old, variable degeneration in the cervical spine is common in the population.

Relating intervertebral displacements to injury requires knowledge of the normal range of motion in the cervical spine. From a survey of radiologic studies of patients, White and Panjabi [30] suggested a limit of cervical spine combined flexion and extension angular range of motion of between 6 and 26 deg. and about 3.5 mm for the upper limit of normal sagittal plane intersegmental translation. If any joint, including those of the spine, exceed their normal range of motion, damage to the interconnecting soft tissues may result. The soft tissues of the facets, including the capsules [7,16,31] and articular cartilage [6,13] have been proposed as locations where damage could occur from intervertebral displacements. Lord, et al, [32] in a double blinded study of patients, showed that 60% of a population with chronic pain after whiplash had symptoms relieved by facet joint injections. These studies give support to the concept that reducing spinal intersegmental motions can reduce the potential for whiplash injury.

Eichburger, et al [8] have proposed that acceleration induced pressure variations occur in the spinal cord during rear impact. However, few victims of relatively low speed rear impact complain of symptoms that might be related to spinal cord pathology. Reported pathologies, from post mortem examination, encompass disc and facet joint lesions. Barnsley, et al [2] performed an extensive review of the pathology of patients with whiplash. They described, facet joint damage, disc injuries, muscle tears, myofacial pain, ligament tears, occasional fractures, and brain hemorrage, with occasional injuries to cervical nerves and the spinal cord. The Quebec task force did identify a level of whiplash associated disorders which included those with neurologic signs [33].

In a study recently presented of 432 low speed rear end impacts, [34], 84 (19%) described arm pain or numbness indicating the possibility of cervical nerve injury. Therefore, as part of this study, but reported elsewhere, we used miniature pressure transducers inserted into the foraminal spaces of the cadaveric specimens at C4-5, C5-6, and C6-7. As with intervertebral displacements, transient pressure changes along the nerve root ganglions during impact were determined and peak pressures correlated with NIC and other measures. However, significant correlations did not result.

These experiments have limitations which have been outlined previously. The specimen donors were quite old and some degeneration was present in all, which caused nonuniformity in the motion response, with some segments being hypermobile and others quite restricted in motion. On the other hand, it is known that the great majority of older adults have some degree of cervical spinal degeneration. A second limitation was not having the torso and seat in the cadaveric tests. We purposely isolated the cervical spine and head restraint by not using a complete cadaver and seat. This reduced the confounding potential of other variables such as how the torso interacted with the seatback. We did tune the impact accelerations so that at the base of the spine they were similar to those experienced by volunteers, and we found that head X and Z accelerations and chest X accelerations of our cadaveric specimens were very similar to those of the volunteers tested on the same apparatus. A third limitation was that we elected to use the same plastic skull for all specimens. Using a plastic skull allowed us to place an accelerometer in its interior at its approximate center of gravity and reduced the variability that would result from having skulls of different weights loading the spines.

In summary, we found the following (i) a cadaveric model using the same head restraint and similar rear impact acceleration does provide responses which are quite similar to less prepared volunteers whose heads hit the head restraint, (ii) spinal intersegmental motions, posterior shear, distraction, and extension angulation are not directly related in the same spine, and (iii) a displacement based criteria, such as Nd, is best for predicting spinal intersegmental motions.

ACKNOWLEDGEMENT

REFERENCES

[1] National Highway Traffic Safety Administration, Federal Register, 66 (3): 967-999, Jan 4, 2001.

[2] Barnsley L, Lord S, Bogduk, Clinical review, whiplash injury, Pain, 58:283-307, 1994.

[3] Barnsley L, Lord SM, Wallis BJ, Bogduk N, The prevalence of chronic cervical zygapophysial joint pain after whiplash, Spine 20:20-26, 1995.

[4] Clark CR, Cervical spine: Neck pain, radiculopathy, and myelopathy, In Instructional Course Lectures, American Academy of Orthopedic Surgeons, Atlanta, GA, Feb 1996.

[5] Deans GT, Magalliard JN, Kerr M, Rutherford WH, Neck sprain-A major cause of disability following car events, Injury, 18:10-12, 1987.

[6] Cusick, J, Pintar FA, Yoganandan, N, Whiplash syndrome, Kinematic factors influencing pain patterns, Spine 26:1252-1258, 2001.

[7] Deng B, Begeman PC, Yang KH, Tashman S, King AI, Kinematics of human cadaver cervical spine during low speed rear-end impacts, STAPP Car Crash Journal, 44:171-188, 2000.

[8] Eichburger, A, Darok, M, Steffan H, Leinzinger PE, Bostrom O, Svensson MY, Pressure measurements in the spinal canal of post-mortem human subjects during rear-end impact and the correlation of results to the neck injury criterion (NIC), World Congress on Whiplash and Associated Disorders, Vancouver, BC, Feb, 1999, pp 346-359, 1999.

[9] Matsushita T, Sato TB, Hirabayashi K, Fujimura S, Asazuma, T, Takatori, X-ray study of the human neck motion due to head inertia loading, Transactions of the Society of Automotive Engineers, 942208, 1994.

[10] McConnell WE, Howard PR, Guzman HM, et al, Analysis of human test subject kinematic responses to low velocity rear end impacts, Transactions of the Society of Automotive Engineers, 930889, 1993

[11] McConnell WE, Howard RP, Van Poppel J, Krause R, Guzman HM, Bomar JB, Raddin JH, Benedict JV, Hatsell CP, Human head and neck kinematics after low velocity rear-end impacts: Understanding whiplash, Transactions of the Society of Automotive Engineers, 952724, 1995.

[12] Mertz HJ, Patrick LM, Investigation of the kinematics and kinetics of whiplash, Transactions of the Society of Automotive Engineers, 670919, 1967.

[13] Ono, K, Kaneoka K, Wittek, A, Kajzer J, Cervical injury mechanism based on the analysis of human cervical vertebral motion and head-neck-torso kinematics during low speed rear impacts, Transactions of the Society of Automotive Engineers, 973340, 1997.

[14] Panjabi MM, Grauer JN, Cholewicki J, Nibu K, Babat LB, Dvorak J, Whiplash trauma: a biomechanical viewpoint, In Whiplash injuries: Current concepts in prevention, diagnosis, and treatment of the cervical whiplash syndrome, ed by Gunzburg R, Szpalski M, Lippincott-Raven, Philadelphia, 1998.

[15] Siegmund GP, King DJ, Lawrence JM, Wheeler JB, Brault JR, Smith TA, Head/neck kinematic response of human subjects in low speed rear-end collisions, Transactions of the Society of Automotive Engineers, 973341, 1997.

[16] Siegmund GP, Myers BS, Davis MB, Bohnet HF, Winkelstein BA, Human cervical motion segment flexibility and facet capsular ligament strain under combined posterior shear, extension, and axial compression, STAPP Car Crash Journal, 44:159-170, 2000.

[17] Szabo TJ, Welcher JB, Anderson RD, Rice MM, Ward JA, Paulo LR, Carpenter NJ, Human occupant kinematic response to low speed rear end impacts, Transactions of the Society of Automotive Engineers, 940532, 1994.

[18] Szabo TJ, Welcher JB, Human subject kinematics and electromyographic activity during low speed rear impacts, Transactions of the Society of Automotive Engineers, 962432, 1996.

[19] Tencer AF, Martin D, Goodwin V, Schaefer G, Mirza S, Do Initial Head Rotation or Head CG Distance Above the Head Restraint Affect Head Kinematics in Response to A Rear-End Impact ? SAE Whiplash 98 conference, Phoenix, AZ, Nov 1988

[20] Tencer AF, Mirza SK, Bensel K, The response of human volunteers to rear-end impacts: The role of head restraint properties, Spine: 22:2432-2442, 2001.

[21] Langwieder K, Hell W, Proposal of an international dynamic test standard for seats/headrestraints, Traffic Injury Prevention, 3:150-158, 2002

[22] Bostrom O, Svensson MY, Aldman B, hansson H, Haland Y, Lovsund P, Seeman T, Suneson A, Saljo A, Ortengren T, A new neck injury criterion candidate based on injury findings in the cervical spine ganglia after experimental neck extension, Proceedings of the 1996 International IRCOBI conference on the Biomechanics of Impacts, pp 123-136, 1996, Dublin, Ireland.

[23] Schmitt K-U, Muser MH, Walz FH, Niederer PF, Nkm- A proposal for a neck protection criterion for low speed rear end impacts, Traffic Injury Prevention, 3:117-126, 2002.

[24] Viano DC, Davidsson J, Neck displacements of volunteers, BioRID P3 and Hybrid III in rear impacts: Implications to whiplash assessments by a neck displacement criterion (NDC), Traffic Injury Prevention, 3:105-116, 2002.

[25] Kleinberger Proceedings of the World Congress on Whiplash Associated Disorders, vancouver, BC, 1999.

[26] Jakobsonb L, Norion H, Suggestions for evaluation of critieria of neck injury protection in rear-end car impacts, Traffic Injury Prevention, 3:216-223, 2002.

[28] Muzzy III WH, Seeman MR, Willems GC, Lustick LS, Bittner AC, The effect of mass distribution parameters on head/neck dynamic response, Transactions of the Society of Automotive Engineers, 861886, 1986.

[29] Thompson JP, Pearce RH, Schechter MT, Adams ME, Tsang IKY, Bishop PB, Preliminary evaluation of a scheme for grading the gross morphology of the human intervertebral disc, Spine, 15:411-415, 1990.

[30] White AA, Panjabi MM, Clinical biomechanics of the spine, 2nd ed, Lippincott, New York, USA.

[31] Panjabi MM, Cholewicki J, Nibu K, Grauer J, Vahldiek M, Capsular ligament stretches during in vitro whiplash simulations, J Spinal Disorders, 11:227-232, 1998.

[32] Lord SM, Barnsley L, Wallis BJ, Bogduk, N, Chronic cervical zygapophyseal joint pain after whiplash, A placebo-controlled prevalence study, Spine, 21:1737-1745, 1996.

[33] Spitzer WO, Skovron ML, Salmi LR, Cassidy JD, Duranceau J, Suissa S, Zeiss E, Scientific monograph of the Quebec task force on whiplash-associated disorders, Spine, Supp 8S, 1995

[34] Tencer AF, Mirza S, Cummings P, Do whiplash victims with neck pain differ from those with neck pain and other symptoms, Proc 45th meeting of the Association for the Advancement of Automotive Medicine, 203-214, 2001.
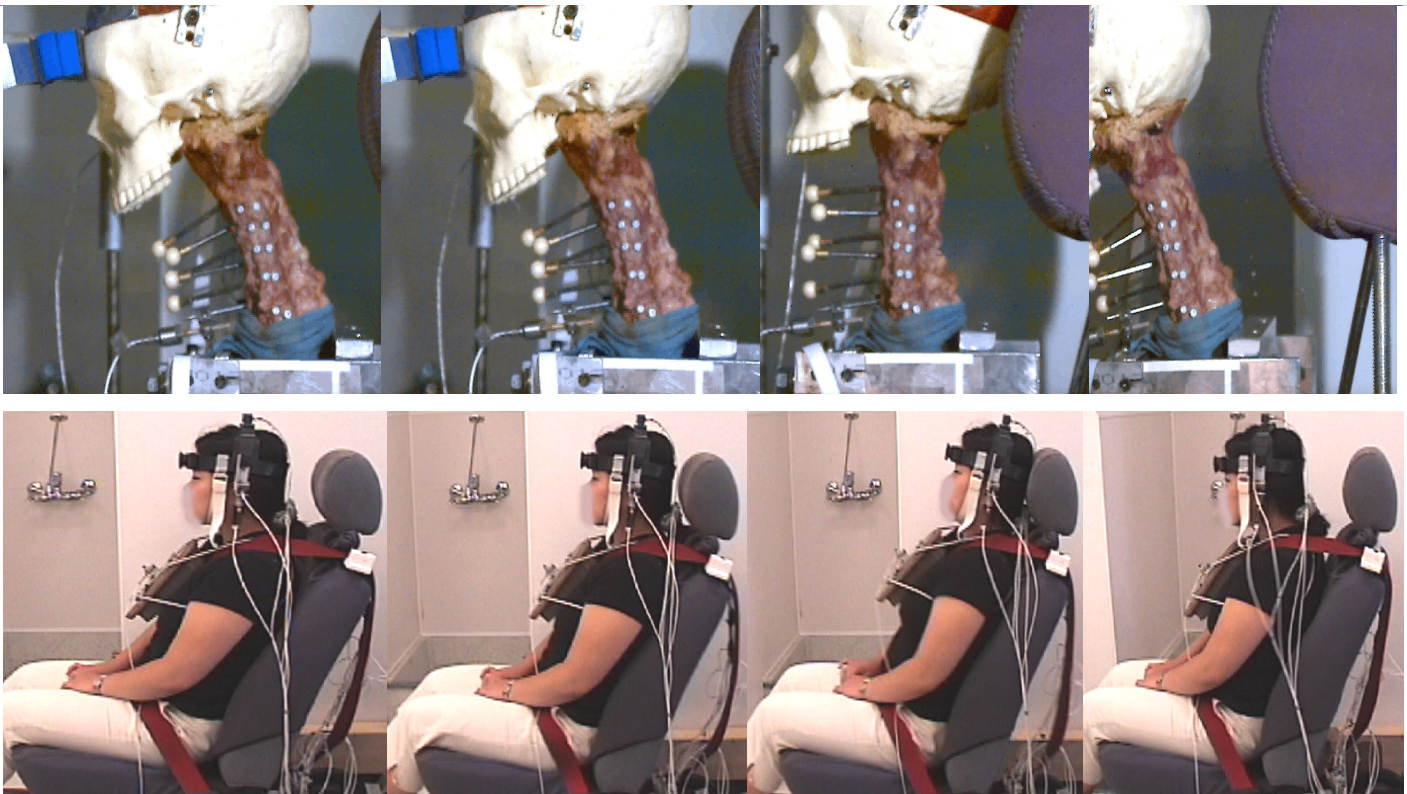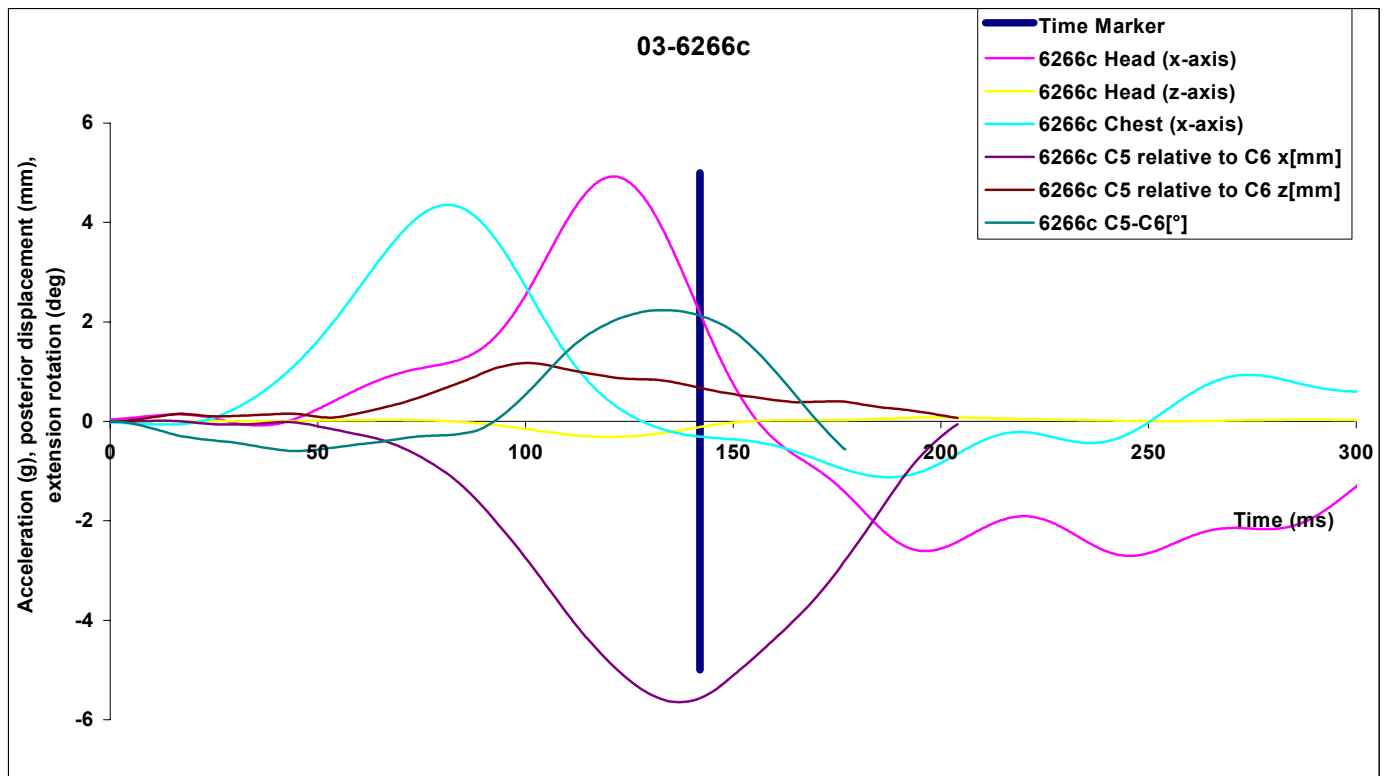
Figure 2 (upper) time history of intersegmental displacements at C5-6, (middle) motion of cadaveric specimen during impact, from left to right, 0 msec, 33 msec, 66 msec, 198 msec, (lower) motion of volunteer at same impact acceleration and approximately the same times.

Table 1.
Characteristics of donors of the cervical spine specimens used in this study.

Specimen number	Gender	Age at death (y)	Degeneration score[1]	Levels with degeneration score of 4 or 5
1	F	63	1.00	
2	F	77	1.33	
3	F	59	2.50	C5-6, C6-7
4	M	82	1.83	C6-7
5	M	85	2.67	C2-3, C3-4
6	F	66	1.00	
7	F	83	3.33	C3-4, C4-5, C6-7
8	F	85	1.83	
9	M	83	4.00	C4-5, C5-6, C6-7
10	M	80	1.17	
11	F	84	1.83	

[1] Grade 1: end plate (EP) uniform thickness, vertebral body (VB) rounded margins, Grade 2, EP irregular thickness, VB pointed margins, Grade 3, EP focal defects, VB chondrophytes, Grade 4, EP fibrocartilage, VB < 2mm osteophytes, Grade 5, EP diffuse sclerosis, VB > 2mm osteophytes

Table 4
Complete set of data used in correlation of injury predictors.

PEAK SHEAR	PEAK ANGLE	PEAK DIST	Nd	ND angle	ND shear	ND dist	NIC MAX	NIC MIN	Nte	Nkm
-6.07	8.270	3.060	1.94	0.78	0.69	0.47	3.76	-8.97	0.12	0.13
-0.48	11.440	0.580	1.18	1.13	0.01	0.04	5.01	-10.33	0.12	0.15
-4.27	5.380	2.500	1.41	0.55	0.53	0.33	6.86	-5.42	0.09	0.13
-8.18	7.250	2.470	1.80	0.81	0.61	0.38	3.69	-10.36	0.13	0.16
-3.72	9.960	1.790	1.16	0.66	0.30	0.20	3.22	-5.17	0.11	0.14
-5.75	13.620	2.780	2.12	1.30	0.49	0.33	4.44	-8.76	0.11	0.13
-5.87	5.250	2.000	1.31	0.56	0.53	0.22	3.52	-9.79	0.09	0.13
-6.74	6.750	2.610	1.42	0.69	0.55	0.19	4.27	-10.79	0.10	0.15
-6.27	5.670	1.400	1.34	0.42	0.59	0.32	4.67	-8.34	0.09	0.13
-8.40	9.330	1.520	1.85	0.84	0.77	0.24	4.76	-9.49	0.09	0.13
-5.45	11.320	3.400	1.70	0.97	0.41	0.32	3.06	-9.77	0.09	0.13
-9.84	11.970	2.320	2.59	1.10	0.92	0.58	4.16	-9.79	0.11	0.14
	12.480		1.21	1.21	0.00	0.00	4.46	-9.60	0.11	0.13
-5.63	4.730	2.060	1.77	0.54	0.69	0.53	3.96	-6.64	0.06	0.09
-7.76	13.870	2.210	2.34	1.26	0.60	0.48	3.98	-12.51	0.12	0.17
-3.46	25.870	1.850	1.79	1.28	0.31	0.21	4.51	-2.38	0.09	0.12
-2.54	15.240	0.370	1.79	1.69	0.07	0.02	4.43	-9.38	0.11	0.13
-7.37	4.190	1.350	1.43	0.55	0.63	0.25	3.51	-9.30	0.09	0.13
-7.99	9.440	2.610	1.75	0.91	0.64	0.20	4.24	-9.42	0.09	0.13
-6.43	7.720	1.580	1.46	0.49	0.59	0.38	3.62	-9.33	0.08	0.12
-8.55	12.570	2.440	2.38	1.22	0.79	0.37	4.16	-9.26	0.09	0.12
-6.26	11.670	2.580	1.88	1.16	0.38	0.33	2.92	-9.72	0.08	0.12
-10.11	10.220	2.990	2.60	1.04	1.01	0.55	8.82	-16.06	0.23	0.27
-2.29	18.430	2.900	1.86	1.60	0.07	0.19	6.67	-7.76	0.20	0.20
-6.55	6.760	4.380	2.16	0.63	0.80	0.73	6.39	-7.50	0.11	0.16
-10.57	8.840	1.720	1.97	0.85	0.84	0.28	7.69	-14.58	0.22	0.28
-6.20	10.270	2.730	2.04	1.09	0.59	0.37	9.66	-8.63	0.17	0.22
-8.56	18.080	4.250	2.90	1.39	0.79	0.72	8.07	-8.18	0.19	0.20
-8.09	6.770	2.130	1.90	0.88	0.73	0.30	6.90	-13.36	0.15	0.22
-7.10	6.540	2.680	1.71	0.78	0.71	0.23	9.80	-12.52	0.15	0.21
-8.09	7.620	2.430	1.60	0.37	0.83	0.40	7.03	-8.88	0.13	0.18
-12.39	11.800	2.370	2.63	1.04	1.17	0.42	9.40	-15.53	0.18	0.26
-8.76	13.560	2.790	2.04	1.14	0.63	0.28	7.22	-14.93	0.18	0.26
-9.03	9.280	2.800	2.26	0.85	0.88	0.54	6.16	-4.87	0.12	0.14
	11.190		1.04	1.04	0.00	0.00	4.57	-5.91	0.10	0.10
-5.61	4.770	4.130	1.83	0.50	0.69	0.64	6.77	-2.34	0.07	0.11
-10.56	5.610	1.800	1.56	0.48	0.76	0.32	6.71	-9.64	0.17	0.21
-5.67	11.330	3.270	2.02	1.17	0.45	0.39	4.97	-3.24	0.14	0.15
-7.55	10.720	4.720	2.51	1.11	0.66	0.74	5.45	-4.65	0.12	0.12
-6.35	5.800	2.500	1.45	0.72	0.50	0.23	5.54	-7.98	0.13	0.19
-7.92	7.290	3.080	1.82	0.91	0.68	0.24	6.88	-7.66	0.11	0.16
-7.27	7.060	2.220	1.07	0.33	0.50	0.25	6.36	-3.15	0.07	0.10
-8.27	4.690	2.000	1.59	0.42	0.82	0.35	6.14	-4.48	0.07	0.11
-7.38	13.190	2.330	1.90	1.18	0.48	0.23	4.72	-8.96	0.12	0.18
-8.71	6.950	3.050	2.09	0.69	0.77	0.63	4.14	-10.18	0.15	0.16
	18.740		1.48	1.48	0.00	0.00	4.14	-8.68	0.10	0.13
-4.20	3.670	2.660	1.44	0.45	0.52	0.47	5.75	-5.21	0.08	0.12
-8.75	11.490	1.330	1.88	0.98	0.64	0.26	4.05	-11.18	0.14	0.18
-3.61	10.520	3.050	1.41	0.79	0.32	0.30	3.69	-7.89	0.13	0.13
-5.52	12.650	1.530	1.99	1.27	0.45	0.27	4.73	-7.44	0.11	0.13
-5.63	4.570	1.890	1.48	0.68	0.49	0.32	3.89	-8.17	0.08	0.11
-7.13	6.780	2.260	1.47	0.69	0.58	0.20	4.68	-10.07	0.10	0.14
-6.21	6.780	1.930	2.16	1.17	0.61	0.39	3.95	-7.54	0.09	0.12
-10.04	14.940	2.780	2.58	1.25	0.92	0.41	4.89	-11.05	0.11	0.16
-6.05	11.790	2.090	1.79	1.14	0.42	0.23	3.28	-9.99	0.10	0.14